^{13}C, ^{14}N and ^{15}N ENDOR measurements on the single substitutional nitrogen centre (P1) in diamond

1994 J. Phys.: Condens. Matter 6 551

(http://iopscience.iop.org/0953-8984/6/2/025)

J. Phys.: Condens. Matter 6 (1994) 551–563. Printed in the UK

^{13}C, ^{14}N and ^{15}N ENDOR measurements on the single substitutional nitrogen centre (P1) in diamond

A Cox, M E Newton and J M Baker
Oxford Physics, Clarendon Laboratory, Parks Road, Oxford OX1 3PU, UK

Received 15 September 1993

Abstract. New ENDOR measurements on the single substitutional nitrogen centre in diamond are reported. The CW-ENDOR mechanism utilizes cross relaxation, and measurements have been made on both ^{14}N and ^{15}N, as well as the first detailed ^{13}C ENDOR study on the isotope at the natural abundance of 1.1%. The change in EPR intensity induced by driving the ^{13}C nuclear transitions was approximately equal to 100% of the EPR intensity of the appropriate ^{13}C hyperfine satellite. The assignment of ^{13}C hyperfine coupling matrices with specific sites is considered, and predictions made about the signs of some of the ^{13}C hyperfine interactions.

1. Introduction

Nitrogen is the most prevalent impurity in diamond. The single substitutional nitrogen centre (P1), has been extensively studied by EPR and ENDOR, and it has long been accepted that the nitrogen forms four bonding orbitals with its neighbouring carbon atoms, whilst the remaining unpaired electron goes into a highly localized antibonding orbital directed along one of the N–C directions. Single substitutional nitrogen is a deep donor, and is not useful as a n-type dopant, but is often intimately involved with other defects and impurities via electron transfer.

In the original EPR paper (Smith *et al* 1959), and subsequently in the calculation by Messmer and Watkins (1973), it was asserted that the trigonal symmetry of the P1 centre was due to a Jahn–Teller distortion. Motional averaging studies (Shul'man *et al* 1967, Loubser and van Ryneveld 1967) which showed thermally induced reorientation of the P1 centre appeared to confirm this assertion. However, estimates of the Jahn–Teller energy based on the reorientation energy (0.7 eV) are suspiciously large. Subsequently, self-consistent calculations (Bachelet *et al* 1981) on the undistorted substitutional nitrogen defect were shown to predict an A_1 antibonding state, contradicting the Messmer and Watkins (1973) calculation of a T_2 state, which is unstable to a Jahn–Teller splitting.

Recent *ab initio* calculations (Kajihara *et al* 1991, and Briddon *et al* 1991), conclude that for the undistorted substitutional nitrogen there is a singly occupied A_1 state in the gap, so that the off-centre distortion cannot be described by manifestation of the Jahn–Teller effect. In fact it is the bonding–antibonding occupancy in one of the N–C bonds which is responsible for the distortion lowering the symmetry to trigonal. Although the recent calculations (Kajihara *et al* 1991, and Briddon *et al* 1991) differ on the details of the distortion of the nitrogen and surrounding carbon atoms, two points are clear: (i) the extension of the unique N–C bond is large, both calculations predict extensions of about 25% over the normal C–C bond length; and (ii) the relaxation of the neighbouring carbon atoms is significant.

0953-8984/94/020551+13$07.50

The following several aspects of single substitutional nitrogen incorporation are currently active areas of research: the optical properties associated with the P1 centre (van Enckevort and Versteegen 1992), growth sector dependent uptake of nitrogen, and modification of the lattice parameter (Lang *et al* 1991), and compensation effects (Mort *et al* 1991). The calculations of Briddon and Jones (1993) have given insight into the origins and structure of the one-phonon IR absorption associated with the P1 centre which is currently attracting considerable attention (Chrenko *et al* 1971, Collins 1980, Collins and Woods 1982, Collins *et al* 1992, Woods *et al* 1990).

Stimulated by the recent experimental and theoretical interest, we have made new ^{13}C, ^{14}N and ^{15}N ENDOR measurements on the P1 centre. It is hoped that the information these measurements provide on the distribution of the unpaired electron and distortion surrounding the nitrogen atom, will encourage further calculations, and ultimately an improved understanding of this defect.

2. Previous EPR and ENDOR measurements

Smith *et al* (1959) first observed the P1 centre, and identified nitrogen because it is the only naturally occurring atom with an almost 100% abundant $I = 1$ isotope. Smith *et al* (1959) also observed ^{13}C satellites from a unique carbon neighbour; the atomic model of a single substitutional nitrogen atom, with a unique N–C bond elongated to accommodate the unpaired electron localized in a N–C antibonding orbital was established. Analysis of the hyperfine coupling with simple theory (Loubser and van Wyk 1978), indicates a localization of 25% of the unpaired electron on the nitrogen, and 67% on the unique carbon.

Subsequent EPR measurements (Loubser and du Preeze 1965), identified weak transitions arising from: (a) forbidden hyperfine transitions, allowing an estimate to be made of the ^{14}N quadrupole interaction; (b) the natural abundance (0.365%) of ^{15}N; and (c) hyperfine satellites from neighbouring ^{13}C nuclei. Cook and Whiffen (1966) and Cook (1966), accurately measured the ^{14}N hyperfine and quadrupole interactions using ENDOR. The dependence of the anisotropic component of the ^{14}N hyperfine interaction and ^{14}N quadrupole interaction on temperature, between 77 and 300 K, is consistent with volume change. Barklie and Guven (1981) were able to resolve ^{13}C couplings with seven neighbouring carbon atoms. Their results (together with the ^{14}N parameters determined by Cook and Whiffen 1966) are given in table 1. The labelling of the possible sites refers to figure 1. Dipolar coupling between distant ^{13}C neighbours and the unpaired electron localized in the unique N–C antibonding orbital, and the distortion of the lattice around the nitrogen are both expected to lower the symmetry of the observed ^{13}C interactions. This was not observed in the EPR even when the linewidth was 7.5 ± 0.4 μT, but is resolved by ENDOR.

3. Experimental studies

3.1. Characterization of the sample

All measurements reported here were made on a synthetic Ib diamond, which had previously been irradiated with 4 MeV electrons (dose 5×10^{18} cm^{-2}), and annealed for 50 hours at 1750 °C, under a stabilizing pressure of 5 GPa. Considerable aggregation of the nitrogen to A centres ([N–N] pair) had taken place (Evans and Qi 1982). The IR absorption spectrum measured for the diamond is shown in figure 2. The IR absorption in the one-phonon region is

Table 1. ^{14}N hyperfine and quadrupole parameters determined by Cook and Whiffen (1966). ^{13}C hyperfine parameters as given by Barklie and Guven (1981). Sites refer to figure 1. Directions of principal values of hyperfine matrices given as $[\theta, \phi]$, where θ is measured from the [001] crystal axis, and ϕ from the [100] axis while rotating about [001].

Atom (site)	Hyperfine and quadrupole interactions (MHz)
C_1 (a)	$A_\parallel = 340.8 \parallel [54.74, 45]$
	$A_\perp = 141.8$
^{14}N	$A_\parallel = 114.03 \parallel [54.74, 45]$
	$A_\perp = 81.33$
	$P_\parallel = -3.97 \parallel [54.74, 45]$
C_2 (d)	$A_\parallel = 41.3 \parallel [54.74, 45]$
	$A_\perp = 32.1$
C_3 (b or c)	$A_\parallel = 23.3 \parallel [54.74, 225]$
	$A_\perp = 26.8$
C_4 (c or b)	$A_\parallel = 14.5 \parallel [54.74, 225]$
	$A_\perp = 11.2$
C_5 (g or e)	$A_\parallel = A_\perp = 8.2$
C_6 (f)	$A_\parallel = A_\perp = 4.1$
C_7 (e or g)	$A_\parallel = A_\perp = 2.7$

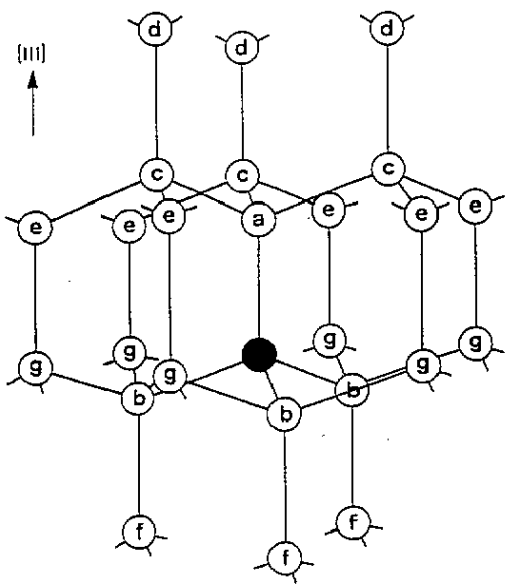

Figure 1. Carbon atom sites around single substitutional nitrogen atom (filled circle). The labelling of carbon atoms refers to notation used in text. Figure adapted from Barklie and Guven (1981).

primarily due to the A and P1 nitrogen centres, although the shoulder at 1332 cm^{-1} indicates the presence of the X component discussed by Lawson and Kanda (1993). From the IR absorption we estimate a P1 concentration of approximately 80 ppm, which is consistent with the EPR measurements.

EPR measurements revealed that as well as the P1 centre the sample also contained the substitutional nickel centre ($[Ni]^-$ Isoya *et al* 1990), as can be seen in figure 4(*a*).

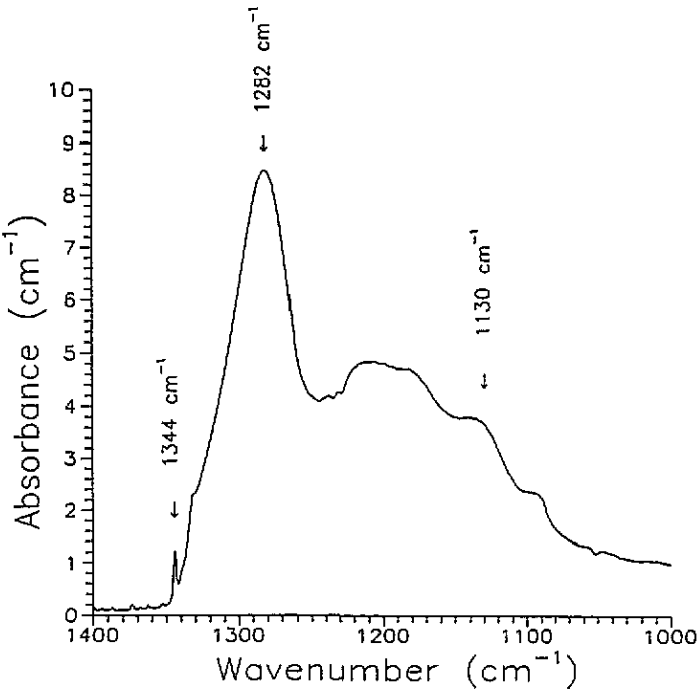

Figure 2. Infrared absorption spectrum showing strong A-centre feature at 1282 cm^{-1} and weaker P1 feature at 1344 and 1130 cm^{-1}.

The nickel ($S = \frac{3}{2}$) is located in a tetrahedral substitutional site, without detectable nearby charge compensation. It has been proposed that the centre is a $[Ni]^-$ ion with electronic configuration $3d^7$. The $[Ni]^-$ concentration was difficult to measure because of saturation and strong cross relaxation to the P1 centre, but we estimate the concentration to be $< 10^{-2}$ times that of the P1 centre. No other centres were detected via EPR.

The isotopes of nitrogen and carbon were present in their natural abundances. We believe that the results reported here are the first detailed ^{13}C ENDOR measurements on this isotope in natural abundance (1.1%) for any defect in diamond (see section 3.3).

3.2. ENDOR cavity and spectrometer

All measurements were made at approximately 9.65 GHz using a TM_{110} ENDOR cavity constructed in the Clarendon Laboratory and described previously (Cox *et al* 1992).

The CW-ENDOR spectrometer (designed and constructed in house), operates with several different detection schemes: (a) modulation of the external magnetic field (10–230 kHz), frequency modulation of the ENDOR RF field (5–1000 Hz), and double phase-sensitive detection; (b) modulation of the external magnetic field (10–230 kHz), unmodulated ENDOR RF, and phase sensitive detection; (c) no magnetic field modulation, frequency modulation of the ENDOR RF field (5–1000 Hz), and phase-sensitive detection (infrequently used); and (d) as (a), but using the enhancement technique described by Newton and Baker (1991b). The variety of detection schemes allows optimal detection of the CW-ENDOR signal under a range of different relaxation conditions.

3.3. Cross relaxation and CW-ENDOR

^{14}N ENDOR for the P1 centre was first reported by Cook and Whiffen (1966) using superheterodyne detection of the EPR, and frequency modulation of the ENDOR RF field.

In this work strong ^{14}N ENDOR signals (signal to noise > 200:1) were detected using detection scheme (b), described above. The other techniques which involved modulation of the ENDOR RF worked very poorly, because of the very long nuclear relaxation times. The ^{14}N ENDOR response, with detection scheme (b) was investigated:

(1) Simple ΔT_1 (T_1 is the spin lattice relaxation time) ENDOR theory predicts that when the $m_I = \pm 1$ EPR transitions are saturated, two different pairs of ENDOR transitions should be observed. Whereas four ENDOR transitions should be observed when the $m_I = 0$ EPR transition is saturated. This is the behaviour usually observed for the P1 centre (Cook 1966), and is useful because it allows determination of the relative signs of the quadrupole and hyperfine interactions. However, for temperatures below 150 K it was found that four ^{14}N ENDOR lines could be detected from the $m_I = \pm 1$ EPR transitions, and none from the $m_I = 0$ EPR transitions.

(2) The ^{14}N ENDOR signals showed the expected dependence with both microwave and RF power.

(3) The ENDOR response reverted to that predicted by simple ΔT_1 ENDOR theory above approximately 170 K, when observing on the $m_I = -1$ EPR transition. Above 170 K ENDOR transitions could be detected from the $m_I = 0$ EPR transitions, and the transition approached the expected relative intensities above about 250 K.

One plausible explanation of observation (1) invokes nitrogen–nitrogen cross relaxation, which occurs via a four spin flip mechanism which exactly conserves Zeeman energy. In this process two spins of the $m_I = 0$ transition make a downward (upward) transition, while a spin belonging to each satellite makes an upward (downward) transition. If one transition is suddenly saturated then the four spin flip mechanism communicates this to the other transitions in a time T_{12}. This process was demonstrated in the beautiful microwave double resonance experiments on the P1 centre by Sorokin *et al* (1960).

Simple rate theory indicates that if T_{12} is much less than T_2, saturating either $m_I = \pm 1$ EPR transitions will produce significant population differences between all nuclear levels. Subsequent saturation of the nuclear transitions short circuits the very slow nuclear relaxation paths, four spin flip cross relaxation readjusts the populations, and all four ENDOR signals are observed from the $m_I = \pm 1$ EPR transitions. The response following application of RF at the resonance frequency of one ^{14}N ENDOR transitions only allowed through cross relaxation is shown in figure 3. As expected the speed of rise and decay are strong functions of microwave saturation, but not of RF power once this is raised to a level sufficient to saturate the nuclear transition. The curves shown are recorded under conditions of fairly low microwave saturation. The steep rise in signal is associated with rapid cross relaxation, and the slow decay with the system coming to a new equilibrium under the influence of spin lattice relaxation and microwave saturation.

On saturating the $m_I = 0$ EPR transition, four spin flip cross relaxation will act to remove population differences between nuclear sublevels, and hence no ENDOR signals are expected, or detected.

The above explanation, although plausible, is undoubtedly an oversimplification. Cross relaxation between the $[Ni]^-$ centre and P1 is well known, (Shul'man and Podzyorei 1975). Above 150 K, the $[Ni]^-$ EPR line broadens rapidly (linewidth goes as T^9) due to fast spin-lattice relaxation. At room temperature the signal is not observable. P1 $\leftrightarrow$ $[Ni]^-$ $\leftrightarrow$ P1 cross relaxation is possible, as well as the P1 $\leftrightarrow$ P1 cross relaxation discussed above. Even

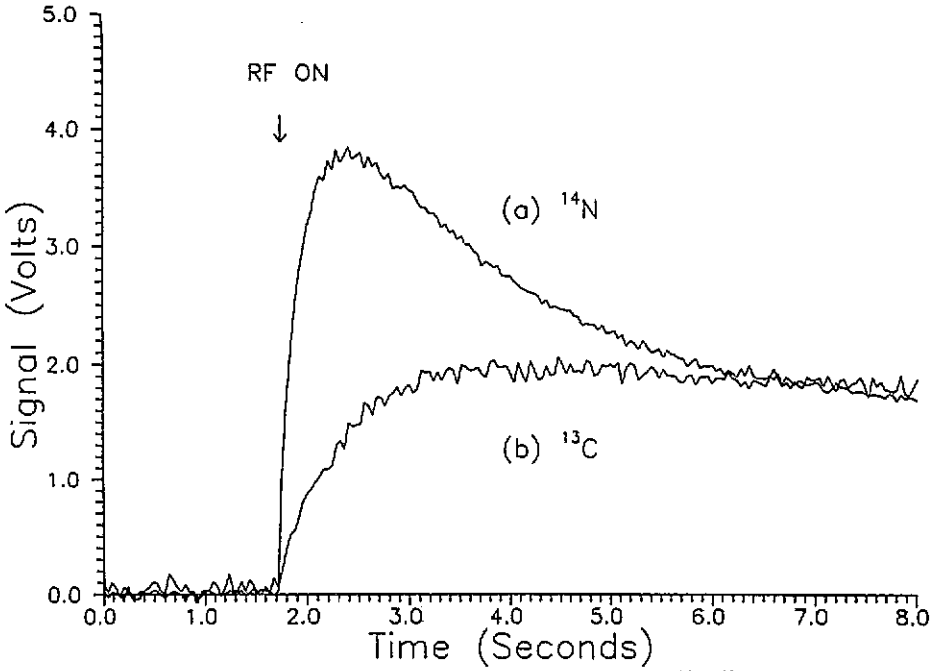

Figure 3. ENDOR response when detecting on $m_I = -1$ ^{14}N–^{12}C EPR transition and applying on resonance ENDOR RF at (a) ^{14}N ENDOR transition not allowed by simple ΔT_1 mechanism, and (b) $^{13}C_a$ ENDOR transition. Microwave power 3 μW, temperature 5 K, microwave frequency 9.65 GHz, and RF power sufficient to saturate ENDOR response.

though in the sample studied here the ratio of [Ni]$^-$ to P1 is small, cross relaxation between the two centres is likely to have a significant effect on the relaxation properties of the P1 centre, because the [Ni]$^-$ is much more strongly coupled to the lattice. Tentative support for this hypothesis is provided by the observations, summarized above in (3), that indicate a change in the dominant ENDOR mechanism in the range 170–220 K, the same range that the [Ni]$^-$ centres shows a marked change in relaxation behaviour. We speculate that above 150 K, T_1 for [Ni]$^-$ is so short that spin coherence is lost rather than transferred in cross relaxation between P1 $\leftrightarrow$ [Ni]$^-$ $\leftrightarrow$ P1, and the ENDOR mechanism due to T_{12} is washed out.

Both ^{13}C, and ^{15}N ENDOR transitions were detected while saturating the main ^{14}N $m_I = \pm 1$ EPR transitions, even though these transitions do not involve any common energy levels. For example, the 1.1% abundance of ^{13}C means that the unique carbon of the P1 centre can be either ^{12}C or ^{13}C, the different combinations ^{14}N–$^{12}C_a$ and ^{14}N–$^{13}C_a$, are strongly coupled, and the $^{13}C_a$ ENDOR transitions can be detected from the ^{14}N–$^{12}C_a$ EPR transition with an ENDOR efficiency of approximately 100% of the ^{13}C EPR signal. The response of ^{14}N–$^{12}C_a$ EPR upon driving a $^{13}C_a$ ENDOR transition is shown in figure 3. It is possible that the cross relaxation observed here is mediated by the [Ni]$^-$ EPR centre.

The ^{13}C ENDOR measurements reported here are only possible because of the 100% ENDOR efficiency. A composite spectrum showing ^{14}N ENDOR, as well as ^{13}C ENDOR from ^{13}C atoms in different sites relative to the nitrogen is shown in figure 4.

Utilization of cross relaxation for ENDOR from defects in diamond is an interesting phenomenon, especially in the light of the remarkable sensitivity achieved. It appears that

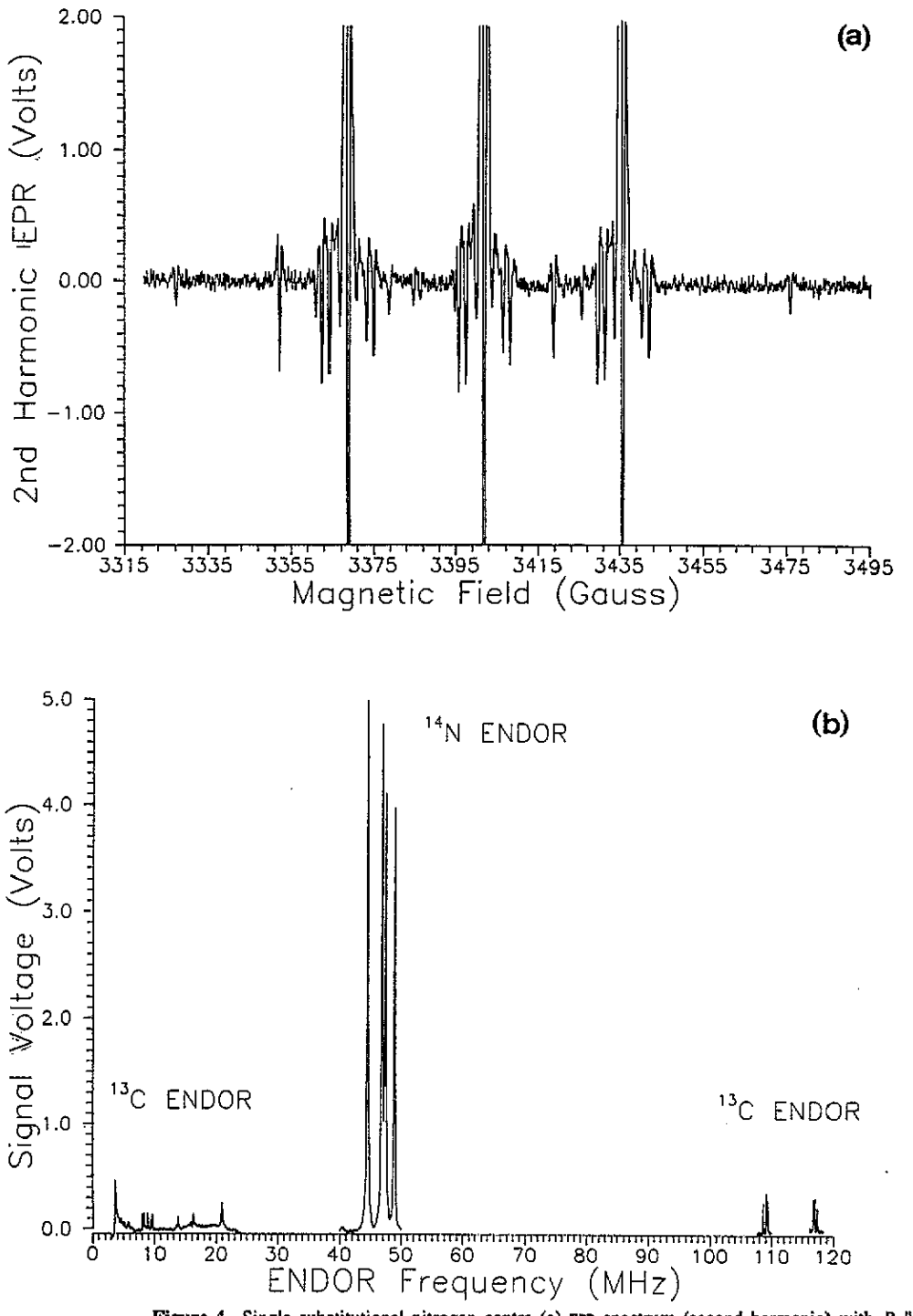

Figure 4. Single substitutional nitrogen centre (a) EPR spectrum (second harmonic) with $B \parallel \langle 100 \rangle$ and (b) ^{13}C and ^{14}N ENDOR with $B \parallel \langle 100 \rangle$. Both spectra were taken at 5 K. The $[Ni]^-$ EPR centre is visible in figure 4(*a*), at approximately 3354.3 G.

nitrogen–nitrogen and nickel–nitrogen cross relaxation are both important. Further work is required to confirm the mechanisms postulated here for the effects observed. For example a strong concentration dependence would be expected. It is of interest to note that no ^{14}N, or ^{13}C ENDOR were detected while saturating the $[Ni]^-$ EPR transition, nor were any resonances detected in any of the experiments which could be associated with ^{61}Ni or ^{13}C atoms neighbouring in the $[Ni]^-$ centre.

4. Results

Detailed ENDOR measurements were made in and around the ⟨100⟩, ⟨111⟩ and ⟨110⟩ directions, at temperatures around 5.0 K. Considerable care was taken to maintain high Zeeman field stability, since signal averaging was run routinely for over 1 hour. The best results were obtained detecting the EPR at twice the field modulation frequency (second harmonic), and not modulating the ENDOR RF frequency.

4.1. ^{14}N, ^{15}N ENDOR

The ^{14}N ENDOR measurements were made on ^{14}N–^{12}C P1 defects, and fitted to an exact solution of the spin Hamiltonian, equation (1), where all terms have their usual meaning, the quadrupole term (P) is absent if $I^{(i)} < 1$, and the summation is carried over the i nuclei coupled to the unpaired electron.

$$H = g\mu_B B \cdot S + \sum_i S \cdot A^{(i)} \cdot I^{(i)} + I^{(i)} \cdot P^{(i)} \cdot I^{(i)} - g_N^{(i)} \mu_N B \cdot I^{(i)}. \quad (1)$$

The parameters obtained, table 2, were in precise agreement with those determined by Cook and Whiffen (1966). Subsequently, weak ENDOR transitions were identified from natural abundance (0.366%) ^{15}N nuclei, in ^{15}N–^{12}C P1 defects. The parameters obtained are given in table 2, and from cursory inspection one can calculate the ratios of $^{14}A_\parallel/^{15}A_\parallel = -0.71390(5)$ and $^{14}A_\perp/^{15}A_\perp = -0.71433(6)$, compared with the ratio of nuclear g factors of -0.71288. The agreement is sufficient to confirm the correct identification of the ^{15}N ENDOR lines, the difference between the two ratios is commonly referred to as a hyperfine anomaly.

Several different mechanisms can give rise to hyperfine anomalies, but all rely on a significant overlap of the nuclear and electronic wavefunctions. Separating $A_\parallel$ and $A_\perp$ into their isotropic and anisotropic components ($A_{2s} = (A_\parallel + 2A_\perp)/3$ and $A_{2p} = (A_\parallel - A_\perp)/3$ respectively), reveals that $^{14}A_{2p}/^{15}A_{2p} = -0.71285(10)$, and $^{14}A_{2s}/^{15}A_{2s} = -0.71416(4)$. $^{14}A_{2p}/^{15}A_{2p}$ is in good agreement with the ratio of nuclear g factors, as expected, because the 2p orbital has a node at the nucleus. $^{14}A_{2s}/^{15}A_{2s}$ is approximately 0.2% larger than the ratio of nuclear g factors. The large hyperfine anomaly is probably due to the difference in zero-point vibration amplitudes of the two nitrogen isotopes in the diamond lattice, such a mechanism was invoked by Feher (1959) to explain the hyperfine anomaly observed for ^6Li and ^7Li in silicon.

4.2. The unique carbon atom

^{13}C ENDOR measurements from ^{14}N–$^{13}C_a$ defects allowed investigation of the ^{13}C hyperfine coupling with the unique carbon neighbour of the nitrogen. The observed ENDOR transitions were fitted to the full Hamiltonian, and the parameters obtained are given in table 2. The accuracy of the ENDOR measurements was an order of magnitude better than that obtained from EPR, and the C_{3v} symmetry was confirmed.

Table 2. ^{14}N, ^{15}N and ^{13}C coupling parameters determined in this work by ENDOR. For further information on the assignment of sites see figure 1 and section 5. Directions of principal values of hyperfine matrices given as $[\theta, \phi]$, where θ is measured from the [001] crystal axis, and ϕ from the [100] axis while rotating about [001].

Atom (site)	Hyperfine and quadrupole interactions (MHz)
C_1 (a)	$A_{\parallel} = 338.171(5) \parallel [54.74, 45]$
	$A_{\parallel} = 139.531(6)$
^{14}N	$A_{\parallel} = 114.032(3) \parallel [54.74, 45]$
	$A_{\perp} = 81.318(2)$
	$P_{\parallel} = -3.973(1) \parallel [54.74, 45]$
^{15}N	$A_{\parallel} = -159.730(7) \parallel [54.74, 45]$
	$A_{\perp} = -113.838(6)$
C_2 (d)	$A_1 = 30.921(5) \parallel [90, 315]$
	$A_2 = 40.292(4) \parallel [58.66, 45]$
	$A_3 = 31.662(4) \parallel [31.34, 225]$
C_3 (c)	$A_1 = 26.488(5) \parallel [90, 315]$
	$A_2 = 22.771(4) \parallel [52.36, 45]$
	$A_3 = 25.319(4) \parallel [37.64, 225]$
C_4 (b)	$A_1 = 10.638(4) \parallel [90, 315]$
	$A_2 = 14.153(4) \parallel [59.19, 45]$
	$A_3 = 10.618(5) \parallel [30.81, 225]$
C_5 (g or e)	$A_1 = 11.757(3) \parallel [71.5, 33.2]$
	$A_2 = 8.579(3) \parallel [138.6, 101.0]$
	$A_3 = 8.122(3) \parallel [55.0, 137.0]$

4.3. Nearest- and next-nearest neighbours

The other carbon neighbours, weakly coupled to the unpaired electron, were also studied. The spectrum taken with $B \parallel \langle 100 \rangle$, figure 5, shows a small splitting for each pair of transitions for each carbon interaction, indicating that the previous reports stating that these couplings had C_{3v} symmetry were incorrect.

From measurements made, hyperfine coupling parameters were determined for three different carbon neighbours, C_2, C_3, and C_4, all of which had σ_h symmetry (i.e. a single {110} mirror plane). The parameters are given in table 2, and the angular variation of the ENDOR transitions of C_4 in a {110} plane are shown in figure 6.

The hyperfine parameters of one more carbon neighbour (C_5) were determined, the angular variation in a {110} plane is shown in figure 7. It is clear that the symmetry is lower, for this hyperfine interaction there is no {110} symmetry plane, and in an arbitrary direction up to 24 distinguishable sites could be resolved. The hyperfine parameters determined from the angular variation are given in table 2 (it was possible to assume that the hyperfine matrix was symmetric because the electronic g-factor for the P1 centre is isotropic). Measurements out of the {110} symmetry plane were used to check the assumptions and assignments made in interpreting the data.

Measurements from 1 to 7.5 MHz revealed many transitions from other more weakly coupled ^{13}C nuclei, but it proved impossible to interpret these resonances unambiguously.

5. Discussion

The ^{14}N ENDOR measurements agree with those previously reported (Cook and Whiffen 1966), but together with the ^{15}N ENDOR measurements show a previously unreported

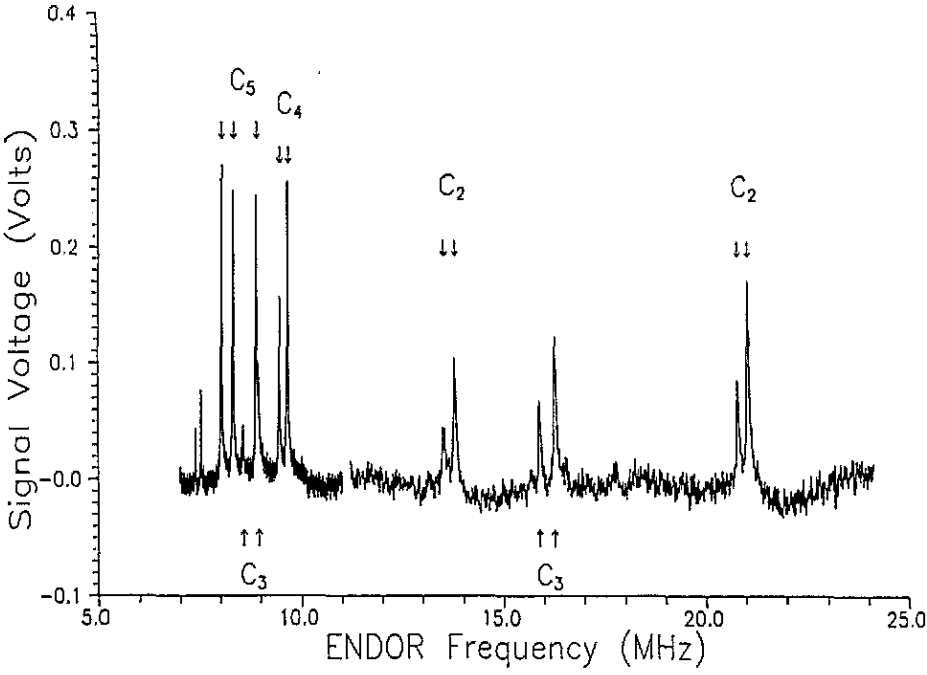

Figure 5. Low-frequency ^{13}C ENDOR from carbon neighbours $C_2 \ldots C_5$ with $B \parallel \langle 100 \rangle$, taken at 5 K.

hyperfine anomaly due to the difference in the zero-point vibration amplitudes of the two isotopes. ^{13}C ENDOR measurements from an atom at site C_a confirm the C_{3v} symmetry of the defect, and give the hyperfine parameters to higher precision. Following the arguments of Coulson (1960), to predict bond angles from the nitrogen and C_a hyperfine interactions, indicates that the N and C atoms are not displaced equivalently.

Positive identification of the sites occupied by $C_2 \ldots C_5$ from the ^{13}C hyperfine parameters determined by ENDOR is not possible. The ENDOR technique used here does not offer the selectivity to enable determination of the orientation of the principal axis of a ^{13}C interaction relative to the unique N–C_a bond axis. It is also impossible from the measurements reported here to determine the sign of the hyperfine interactions $C_2 \ldots C_5$ *relative to that for* C_a. *Localization of unpaired electrons on* $C_2 \ldots C_5$ *in an* sp^n *orbital* would give rise to an interaction the same sign as that for C_a. Spin polarization could contribute negatively or positively depending on the site. Distant dipolar coupling between a carbon neighbour and the unpaired electron localized in the N–C_a antibonding orbital is expected to be important for nearest neighbours. A precise calculation would require a sum over the unpaired electron distribution and has not been attempted here. The following assignments are based on the data presented here, and previous EPR and ENDOR studies.

C_2: Bower and Symons (1966), and Barklie and Guven (1981) determined that C_2 was axially symmetric about the N–C_a direction, and the former proposed that since the unpaired electron density is greater on C_a than N, C_2 should be assigned to site d, hyperconjugation being responsible for the size of this interaction. ^{13}C ENDOR measurements show that C_2 is almost axially symmetric, but tilted from [111] (presumed the undistorted C_d–C_c bond axis) by 3.9°. This magnitude of deformation can be readily explained by distortion around the nitrogen and distant dipolar coupling, and we see no reason to question the assignment

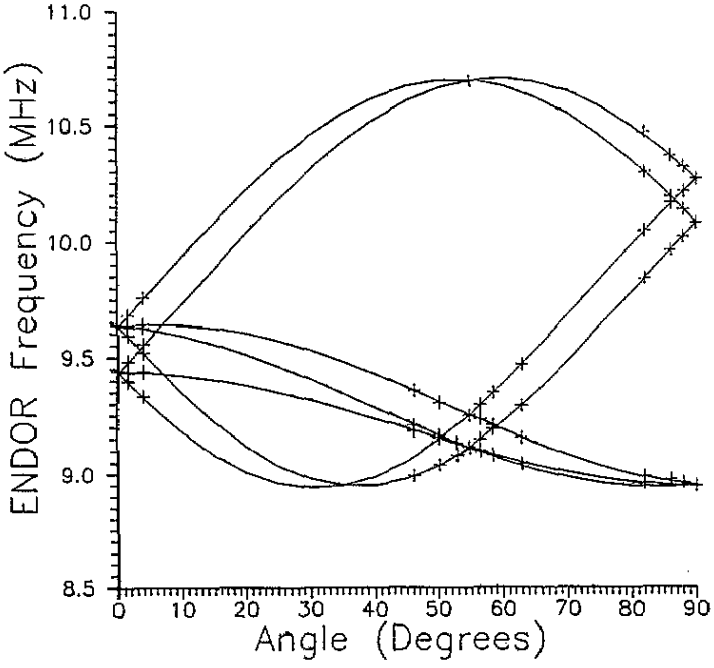

Figure 6. ^{13}C ENDOR angular variation in (110) plane, from neighbour C_4.

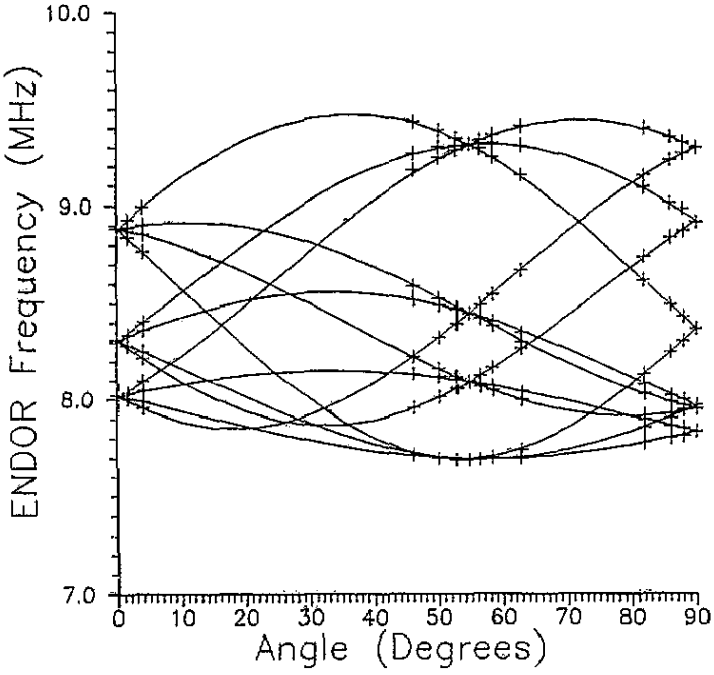

Figure 7. ^{13}C ENDOR angular variation in (110) plane, from neighbour C_5.

of C_d with C_2.

C_3 and C_4: Barklie and Guven (1981) determined that C_3 and C_4 were both axially symmetric about a [111] direction that was not parallel to the N–C_a direction, and hence assigned C_3 (C_4) to site b or c. The hyperfine parameters determined by ENDOR are given in table 2, C_4 is axially symmetric but tilted from [111] (presumed the undistorted C_b–N bond axis) by 4.5°, where as C_3 is only very approximately axially symmetric, and the principal component is tilted from [111] (presumed the undistorted C_b–C_a bond axis) by −2.3°.

For C_3, $A_\parallel$ is less than $A_\perp$, which is unique amongst the interactions measured, but reminiscent of the hyperfine interaction measured for the N^+ of the N1 centre: N_1–C–N_2^+ (Cox *et al* 1992). The small negative value of A_{2s} for the N^+ resulted from a partial cancellation between a negative indirect contribution from spin polarization and a positive direct contribution. The anisotropic component of the hyperfine interaction for N^+ was much smaller than the dipolar interaction between the unpaired electron in the N_1–C and the $^{14}N_2$ nucleus, but consistent with a reasonable value of A_{2p}. Without assuming that the hyperfine interaction of C_3 is negative, it does not seem to be possible to explain the measurements satisfactorily. Calculations of the distant dipolar contribution, and the residual A_{2p}, support the assignment of C_b to C_3. Hence, C_4 can be assigned to C_c. It is expected that the sign of the hyperfine interaction of C_4 is positive.

C_5: The low symmetry of C_5 is consistent with sites C_e or C_g. Work on the W7 centre (N_1–C–C–N_2^+ Newton and Baker 1991a,b) provides accurate coupling parameters for a N^+ atom at site C_e relative to a P1-like N_1–C unit. Similarities in the principal directions of the $^{14}N_2$ and C_5 hyperfine matrices, lead us to suggest tentatively that C_5 can be assigned to C_e. The relatively large hyperfine coupling of N^+ (A_{2s} = 14.53 MHz) in this site may be due to the extra positive charge of N^+ compared to a carbon atom.

C_f and C_g: No hyperfine matrices have been identified that can be associated with C_f and C_g. The hyperfine interaction for C_f should have σ_h symmetry, and C_g the same symmetry as C_e. It is probable that these couplings are weak, and the resonances occur amongst the many unassigned low-frequency ENDOR lines.

We have accurately determined the symmetry and magnitudes of the hyperfine interactions $C_2 \ldots C_5$, and associated these specific sites. We believe that the ambiguity in assigning C_3 and C_4 has been resolved, which prompts predictions of the signs of these interactions. We hope that this will stimulate calculation of the hyperfine coupling parameters. An obvious extension of this work is the determination of the relative signs of the ^{13}C hyperfine couplings, which may be possible in a conventional double-ENDOR (TRIPLE) experiment. The 100% ENDOR efficiency is an exciting discovery, especially if it proves applicable to other investigations.

Acknowledgments

We are grateful to Dr S Satoh of Sumitomo Electric Industries, and Dr A Collins of Kings College for the loan of the sample used in this work. AC thanks the Science and Engineering Research Council for a maintenance grant, and De Beers for partial financial support. We thank Professor J A Weil, Dr D G McGavin and Dr M J Momborquette for the simulation and fitting the software EPR.FOR, and Dr R J Caveney and his associates at the Diamond Research Laboratory, De Beers Industrial Diamond Division, Johannesburg, for their continued interest in the research program.

References

Bachelet G B, Baraff B A and Schluter M 1981 *Phys. Rev.* B **24** 4736

Barklie R C and Guven J 1981 *J. Phys. C: Solid State Phys.* **14** 3621

Bower H and Symons M C R 1966 *Nature* **210** 103

Briddon P R, Heggie M I and Jones R 1991 *Proc. 2nd Int. Conf. on New Diamond Science and Technology (Washington, DC, 1990)* ed R Messier, T J Glass, J E Butler and R Roy (Pittsburgh, PA: Materials Research Society) p 63

Briddon P R and Jones R 1993 *Physica* B **185** 179

Chrenko R M, Tuft R E and Strong H M 1971 *Nature* **270** 141

Collins A T 1989 *J. Phys. C: Solid State Phys.* **13** 2641

Collins A T, Woad P J, Woods G S and Kanda H 1992 *Diamond Conference (Cambridge, UK)* (Johannesburg: De Beers Industrial Diamond Division) p 40

Collins A T and Woods G S 1982 *Phil. Mag* B **46** 77

Cook R J 1966 *J. Sci. Instrum.* **43** 548

Cook R J and Whiffen D H 1966 *Proc. R. Soc.* A **295** 99

Coulson C A 1960 *Valence* (Oxford: Oxford University Press) ch 8

Cox A, Newton M E and Baker J M 1992 *J. Phys.: Condens. Matter* **4** 8119

Evans T and Qi Z 1982 *Proc. R. Soc.* A **381** 159

Feher G 1959 *Phys. Rev.* **114** 1219

Isoya J, Kanda H, Norris J R, Tang J and Bowman M K 1990 *Phys. Rev.* B **41** 3905

Kajihara S A, Antonelli A, Bernholc J and Car R 1991 *Phys. Rev. Lett.* **66** 2010

Lang A R, Moore M, Makepeace A P W, Wierzchowski W and Welbourn C M 1991 *Phil. Trans. R. Soc.* A **337** 497

Lawson S C and Kanda H 1993 *J. Appl. Phys.* **73** 3967

Loubser J H N and du Preez L 1965 *Br. J. Appl. Phys.* **16** 457

Loubser J H N and van Ryneveld W P 1967 *Br. J. Appl. Phys.* **18** 1029

Loubser J H N and van Wyk J A 1978 *Rep. Prog. Phys.* **41** 1201

Messmer R P and Watkins G D 1973 *Phys. Rev.* B **7** 2568

Mort J, Machonkin M A and Okumura K 1991 *Appl. Phys. Lett.* **59** 3148

Newton M E and Baker J M 1991a *J. Phys.: Condens. Matter* **3** 3605

—— 1991b *J. Phys.: Condens. Matter* **3** 3591

Shul'man L A and Podzyorei G 1975 *Sov. Phys.–Solid State* **16** 1377

Shul'man L A, Zaritskii I M and Podzyarei G A 1967 *Sov. Phys.–Solid State* **8** 1842

Smith W V, Sorokin P P, Gelles I L and Lasher G J 1959 *Phys. Rev.* **115** 1546

Sorokin P P, Lasher G J and Gelles I L 1960 *Phys. Rev.* **118** 939

van Enckevort W J P and Versteegen E H 1992 *J. Phys.: Condens. Matter* **4** 2361